Supplemental Material

Representativeness of the IAGOS airborne measurements in the lower troposphere

H. Petetin[1,*], M., Jeoffrion[1], B. Sauvage[1], G. Athier[1], R. Blot[1], D. Boulanger[2], H. Clark[1], J.-M. Cousin[1], F. Gheusi[1], P. Nedelec[1], M., Steinbacher[3], V. Thouret[1]

[1] Laboratoire d'Aérologie, Université de Toulouse, CNRS, UPS, Toulouse, France

[2] Observatoire Midi-Pyrénées, Université de Toulouse, CNRS, UPS, Toulouse, France

[3] Empa-Swiss Federal Laboratories for Materials Science and Technology, Dübendorf, Switzerland

*Corresponding author: H. Petetin (hervepetetin@gmail.com)

List of Contents :

Figure S-1: Location of the IAGOS airborne observations at the Frankfurt airport, coloured depending on the altitude between 0 and 750 m ASL. The grey area corresponds to the Frankfurt city. (Page 4)

Figure S-2: Location of the IAGOS airborne observations at the Vienna airport, coloured depending on the altitude between 0 and 750 m ASL. The grey area corresponds to the Vienna city. (Page 5)

Figure S-3: Location of the IAGOS airborne observations at Paris airports, coloured depending on the altitude between 0 and 750 m ASL. The grey area corresponds to the Paris city (excluding all the suburbs). IAGOS observations are available at two airports: mostly at the Charles-de-Gaulle airport at north, and a few other at the Orly airport at south. (Page 6)

Figure S-4: Monthly time series of CO mixing ratios at Frankfurt. At both GAW and AQN surface stations, monthly data are calculated taking into account only the hourly data when IAGOS flights took place. (Page 7)

Figure S-5: Monthly time series of O_3 mixing ratios at Frankfurt. At both GAW and AQN surface stations, monthly data are calculated taking into account only the hourly data when IAGOS flights took place. (Page 8)

Figure S-6: Relative annual trends of O_3 mixing ratios at Frankfurt, over the period 2002-2012. Trends are calculated by linear regression based on the time series of annual averages. Annual averages are defined only when data are available during all four seasons. Uncertainties are shown at a 95% confidence level. Annual trends of O_3 in most of these datasets are not statistically significant, the only few exceptions being found among the GAW stations (but these trends are low and only poorly significant). (Page 9)

Figure S-7: Orientation of the aircraft against the wind direction at Frankfurt. Only the concomitant landings and take-offs over a time window of 30 min are included. The wind direction is averaged over the first 100 m. Three orientations are available at the Frankfurt airport: 70° and 250° (3 runways, for both take-offs and landings), and 180° (1 runway, only for take-offs). While a wind direction of 90° indicates a wind blowing from east to west, the aircraft angle during both landings and take-offs is here calculated so that an angle of 90°

corresponds to an aircraft flying from east to west (which makes the comparisons with the wind direction easier since aircraft are expected to take-off and land upwind). The Figure illustrates that there are many exceptions in which landings and take-offs are not performed upwind. (Page 10)

Figure S-8: Distribution of the hourly CO (top panel) and O_3 (bottom panel) mixing ratios at the GAW (Global Atmospheric Watch) and AQN (Air Quality Network) surface stations and at different IAGOS altitude levels at Vienna. The Figure shows the 1st, 25th, 50th, 75th and 99th percentiles (box-and-whisker) and the mean (black point). As for the Frankfurt city, the strongest CO mixing ratios are found at traffic stations. Close to the surface, IAGOS data are in close agreement with urban background stations, while higher in altitude, they get closer to the mixing ratios measured at GAW regional stations. Similar results are found with O_3. (Page 11)

Figure S-9: CO (top panel) and O_3 (bottom panel) mixing ratios versus altitude, as given by IAGOS and surface stations at Vienna. The grey area indicates the elevation of the Vienna (180 m) airport. The Figure shows the mean (points) and the 5th and 95th percentiles (horizontal lines). This Fig. highlights a good agreement between IAGOS and surface stations except at traffic stations (for CO). (Page 12)

Figure S-10: Correlation between the IAGOS observations at several altitudes and the surface measurements, at Vienna. Correlations are calculated for the hourly (top panels) and daily (bottom panels) data, for CO (left panels) and O_3 (right panels). For clarity, only the name of GAW stations is written. For each GAW station and for the rural background station, the elevation is indicated on the corresponding curves by open circles with a cross. The altitude of the Vienna (180 m) airport is indicated in grey. Note that as previously indicated, the altitude of IAGOS measurements is deduced from the pressure, which explains that some points may have a barometric altitude below the actual airport elevation (e.g. presence of strong low-pressure systems). For CO, the correlations between IAGOS and AQN surface stations are the strongest close to the surface and decrease with altitude. Conversely, the correlations between IAGOS and GAW stations usually reach a flat maximum at an altitude that roughly corresponds to the elevation of the GAW surface station. For O_3, the correlation between IAGOS and AQN stations is also decreasing with altitude but more progressively. (Page 13)

Figure S-11: Distribution of the CO (top panel) and O_3 (bottom panel) hourly mixing ratios at Paris. The Figure shows the 1st, 25th, 50th, 75th and 99th percentiles (box-and-whisker) and the mean (black point). A strong CO pollution is observed at traffic stations. Although much lower, the CO mixing ratios measured at urban background stations remain higher than the mixing ratios observed by IAGOS close to the surface. However, the O_3 mixing ratios measured by IAGOS close to the surface are consistent with the observations at urban and rural background stations. Higher in altitude, IAGOS O_3 observations get closer to the mixing ratios measured at GAW regional stations. (Page 14)

Figure S-12: CO (top panel) and O_3 (bottom panel) mixing ratios versus altitude, as given by IAGOS and surface stations at Paris. The grey area indicates the elevation of the Paris airport (119 m). The Figure shows the mean (points) and the 5th and 95th percentiles (horizontal lines; only for GAW and IAGOS, for clarity). As at Frankfurt and Vienna, a good agreement is found between the different datasets when plotted against altitude. (Page 15)

Figure S-13: Correlation between the IAGOS observations at several altitudes and the surface

measurements, at Paris. The correlations are calculated for the hourly (top panels) and daily (bottom panels) data, for CO (left panels) and O_3 (right panels). For clarity, only the name of GAW stations is written. For each GAW station and for the rural background station, the elevation is indicated on the corresponding curves by open circles with a cross. The correlation profiles at Paris are more noisy and complex than at Frankfurt and Vienna, which may be partly due to the lower number of data. Although higher close to the surface (with exceptions at a few stations), the correlations on CO between IAGOS and AQN surface stations are very low. They are slightly higher between IAGOS and GAW station in altitude. For O_3, correlations between IAGOS and surface stations are highest close to the surface and decrease with altitude. Contrary to Frankfurt and Vienna, the altitude of maximum correlation on O_3 between IAGOS and GAW usually does not coincide with the elevation of the station. The larger distance between Paris and GAW stations may partly explain these differences. (Page 16)

Table S-1: Description of the surface stations. (Page 17)

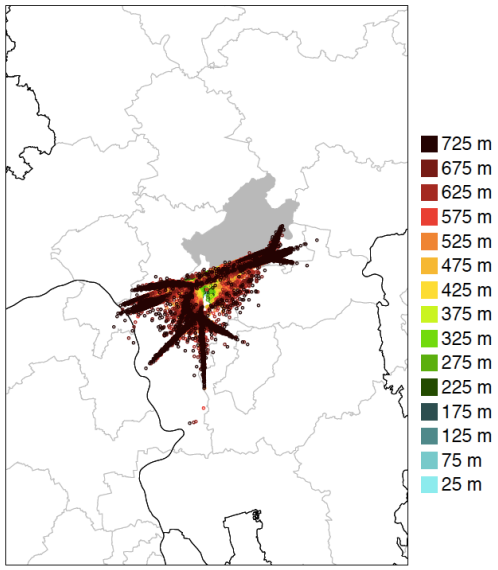

Figure S-1: Location of the IAGOS airborne observations at the Frankfurt airport, coloured depending on the altitude between 0 and 750 m ASL. The grey area corresponds to the Frankfurt city.

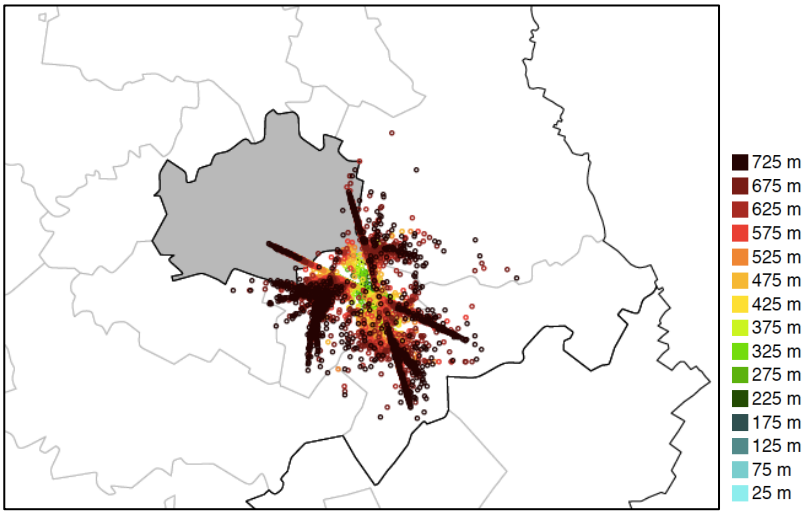

Figure S-2: Location of the IAGOS airborne observations at the Vienna airport, coloured depending on the altitude between 0 and 750 m ASL. The grey area corresponds to the Vienna city.

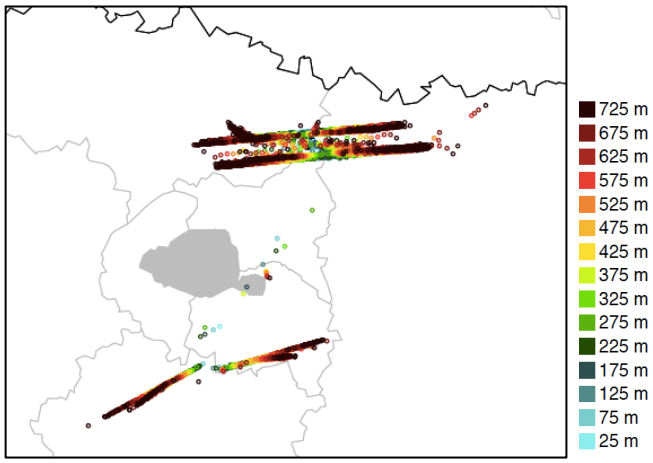

Figure S-3: Location of the IAGOS airborne observations at Paris airports, coloured depending on the altitude between 0 and 750 m ASL. The grey area corresponds to the Paris city (excluding all the suburbs). IAGOS observations are available at two airports: mostly at the Charles-de-Gaulle airport at north, and a few other at the Orly airport at south.

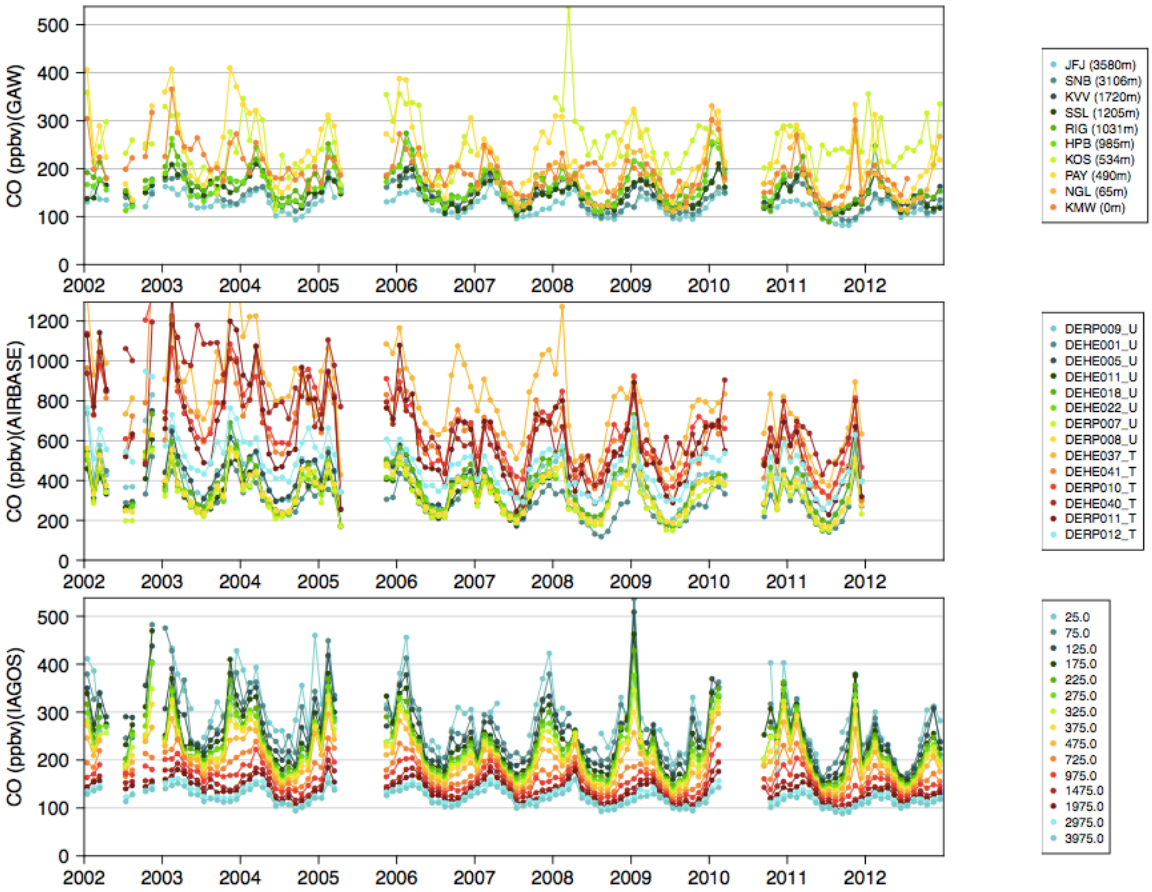

Figure S-4: Monthly time series of CO mixing ratios at Frankfurt. At both GAW and AQN surface stations, monthly data are calculated taking into account only the hourly data when IAGOS flights took place.

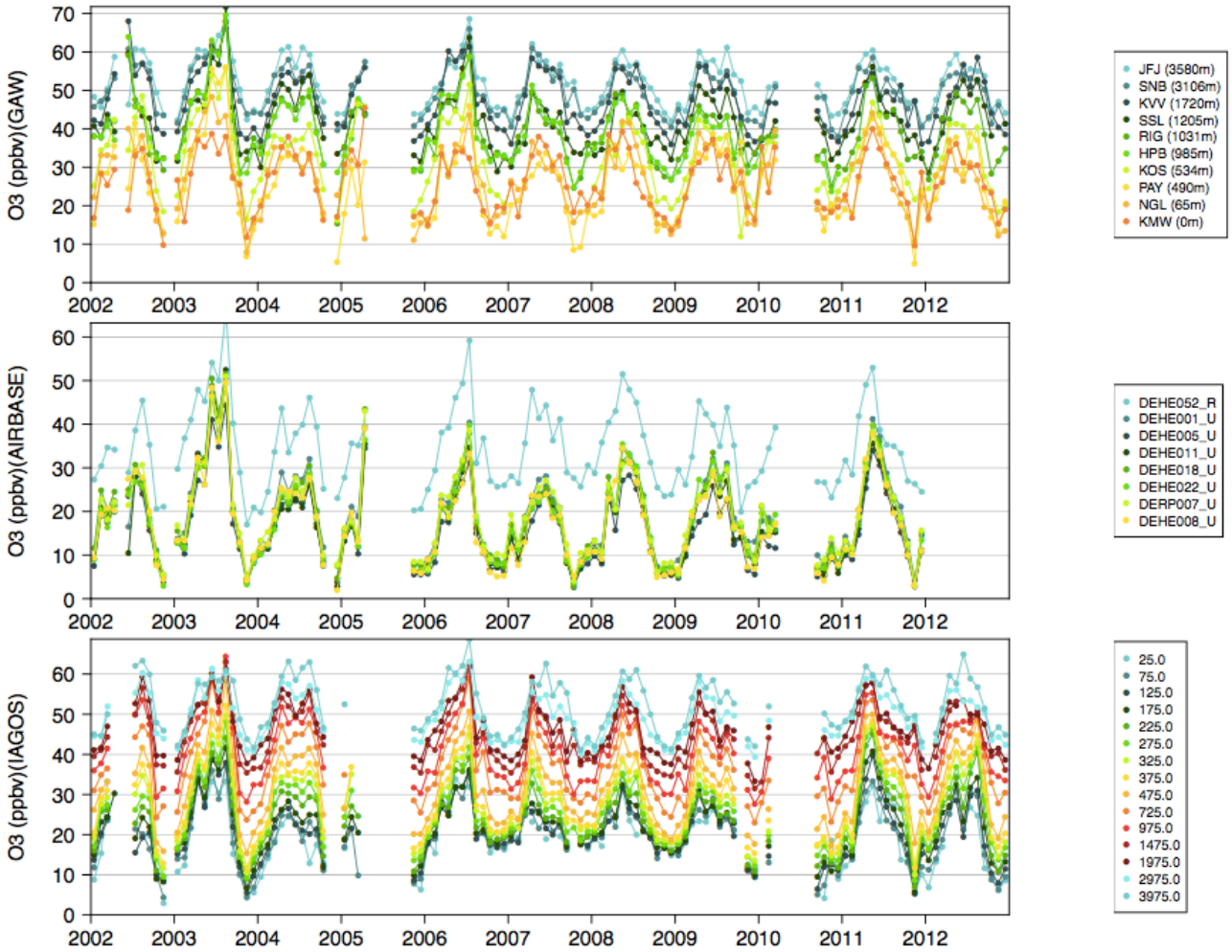

Figure S-5: Monthly time series of O_3 mixing ratios at Frankfurt. At both GAW and AQN surface stations, monthly data are calculated taking into account only the hourly data when IAGOS flights took place.

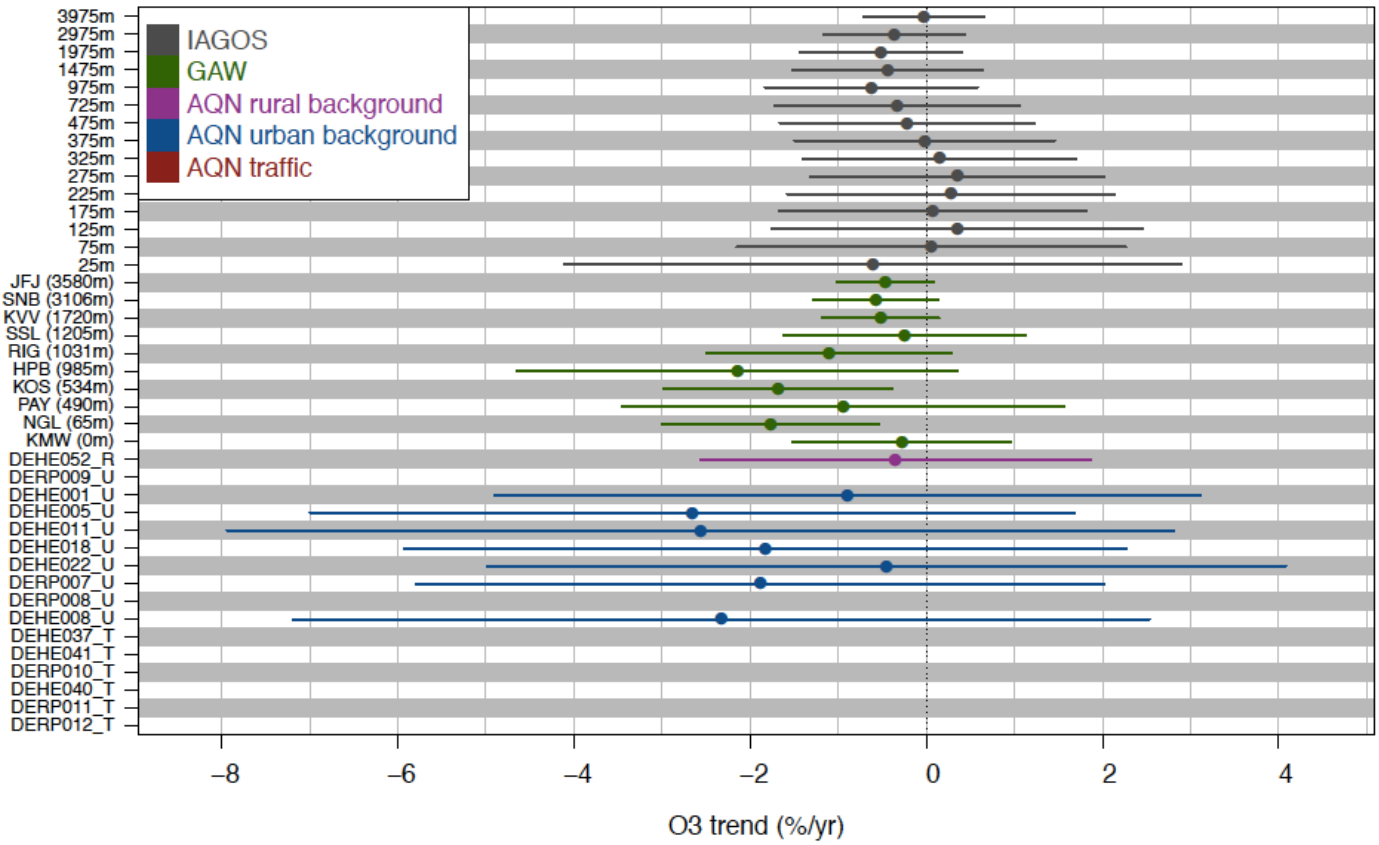

Figure S-6: Relative annual trends of O_3 mixing ratios at Frankfurt, over the period 2002-2012. Trends are calculated by linear regression based on the time series of annual averages. Annual averages are defined only when data are available during all four seasons. Uncertainties are shown at a 95% confidence level. Annual trends of O_3 in most of these datasets are not statistically significant, the only few exceptions being found among the GAW stations (but these trends are low and only poorly significant).

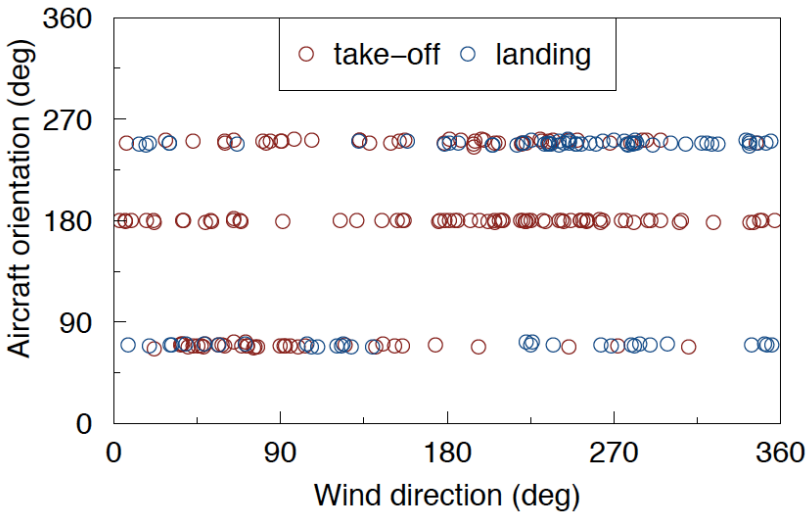

Figure S-7: Orientation of the aircraft against the wind direction at Frankfurt. Only the concomitant landings and take-offs over a time window of 30 min are included. The wind direction is averaged over the first 100 m. Three orientations are available at the Frankfurt airport: 70° and 250° (3 runways, for both take-offs and landings), and 180° (1 runway, only for take-offs). While a wind direction of 90° indicates a wind blowing from east to west, the aircraft angle during both landings and take-offs is here calculated so that an angle of 90° corresponds to an aircraft flying from east to west (which makes the comparisons with the wind direction easier since aircraft are expected to take-off and land upwind). The Figure illustrates that there are many exceptions in which landings and take-offs are not performed upwind.

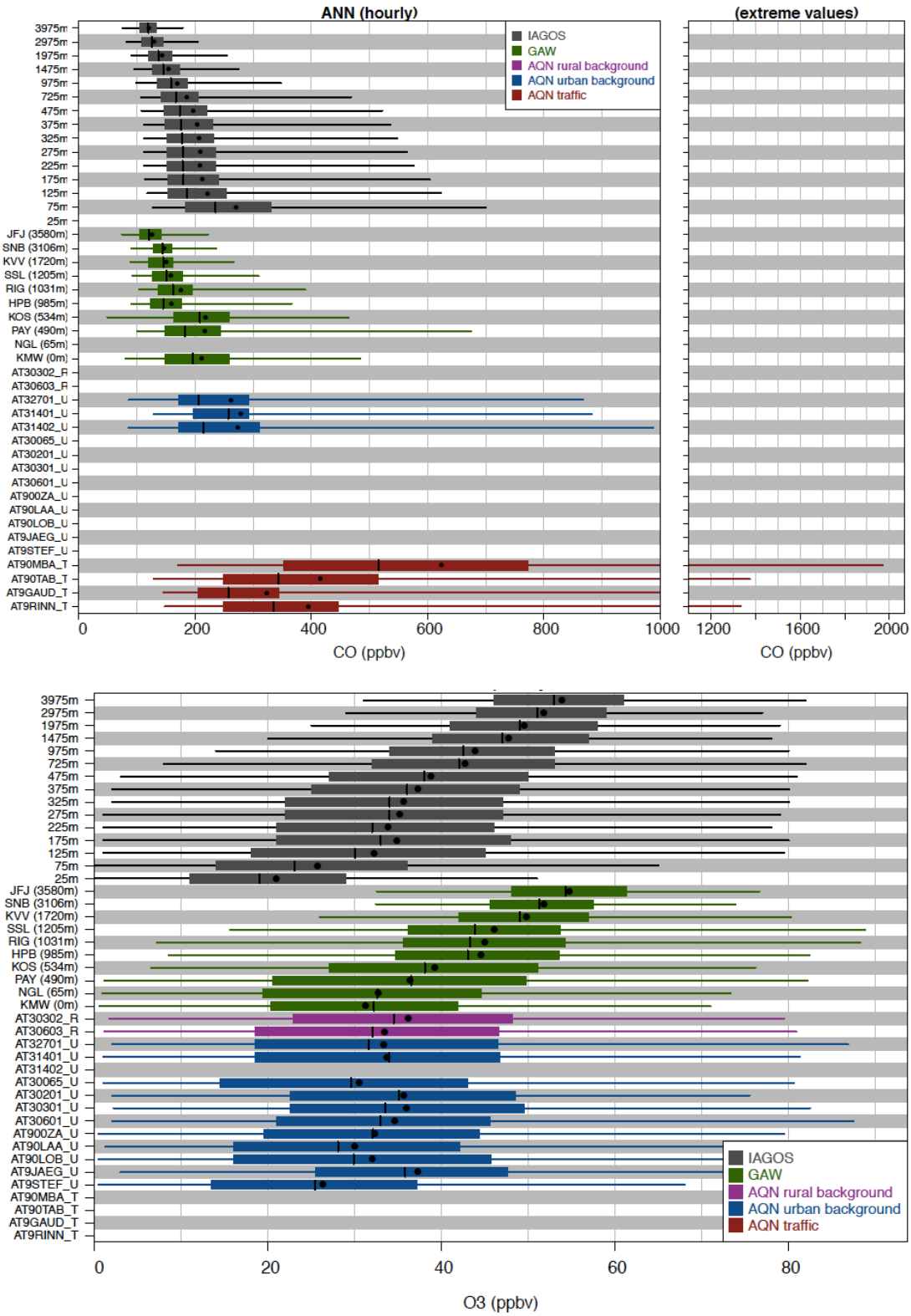

Figure S-8: Distribution of the hourly CO (top panel) and O_3 (bottom panel) mixing ratios at the GAW (Global Atmospheric Watch) and AQN (Air Quality Network) surface stations and at different IAGOS altitude levels at Vienna. The Figure shows the 1st, 25th, 50th, 75th and 99th percentiles (box-and-whisker) and the mean (black point). As for the Frankfurt city, the strongest CO mixing ratios are found at traffic stations. Close to the surface, IAGOS data are in close agreement with urban background stations, while higher in altitude, they get closer to the mixing ratios measured at GAW regional stations. Similar results are found with O_3.

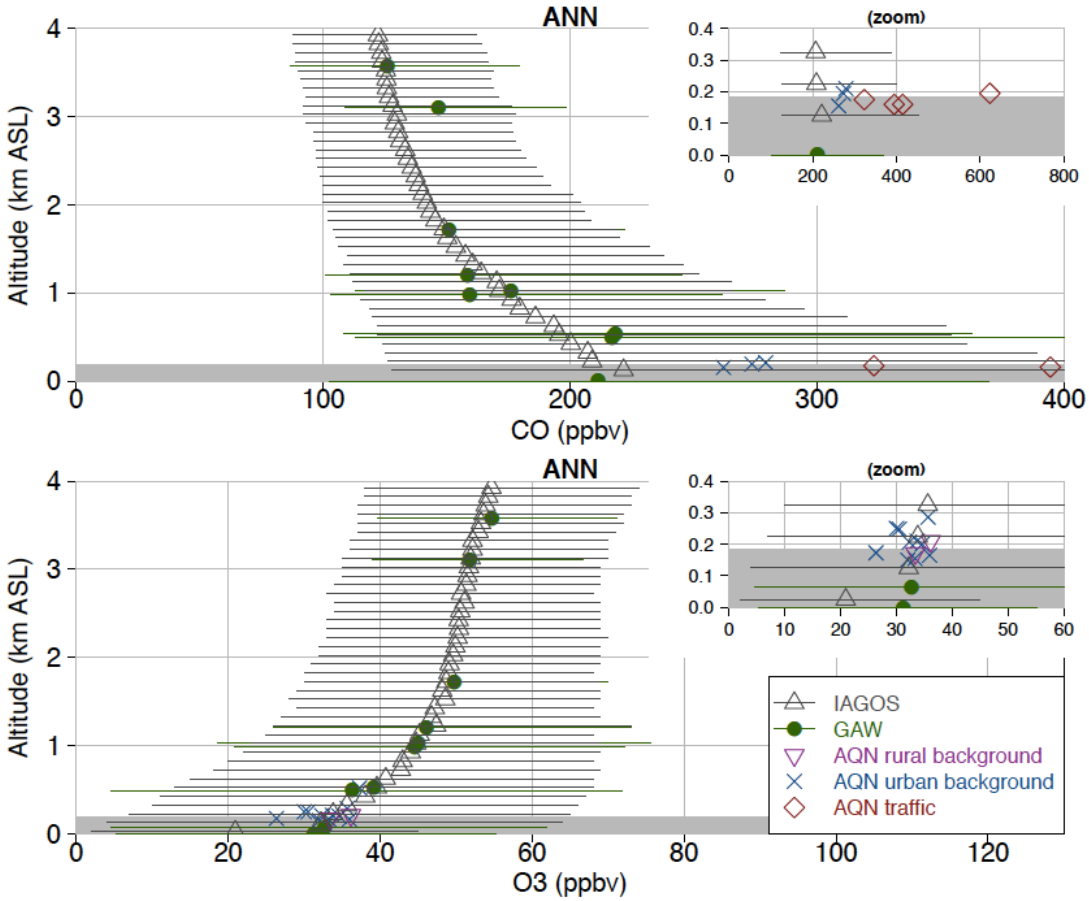

Figure S-9: CO (top panel) and O_3 (bottom panel) mixing ratios versus altitude, as given by IAGOS and surface stations at Vienna. The grey area indicates the elevation of the Vienna (180 m) airport. The Figure shows the mean (points) and the 5th and 95th percentiles (horizontal lines). This Fig. highlights a good agreement between IAGOS and surface stations except at traffic stations (for CO).

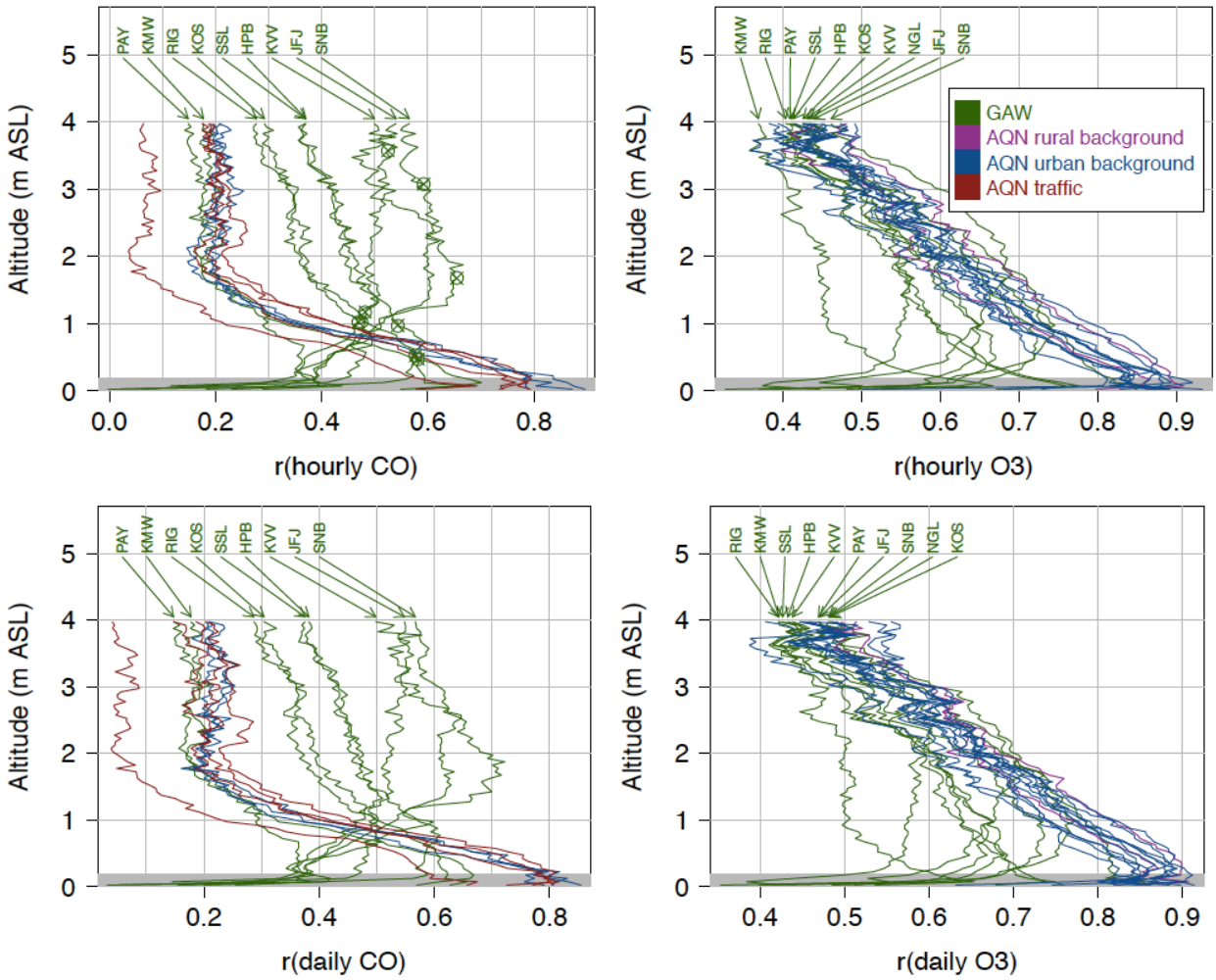

Figure S-10: Correlation between the IAGOS observations at several altitudes and the surface measurements, at Vienna. Correlations are calculated for the hourly (top panels) and daily (bottom panels) data, for CO (left panels) and O_3 (right panels). For clarity, only the name of GAW stations is written. For each GAW station and for the rural background station, the elevation is indicated on the corresponding curves by open circles with a cross. The altitude of the Vienna (180 m) airport is indicated in grey. Note that as previously indicated, the altitude of IAGOS measurements is deduced from the pressure, which explains that some points may have a barometric altitude below the actual airport elevation (e.g. presence of strong low-pressure systems). For CO, the correlations between IAGOS and AQN surface stations are the strongest close to the surface and decrease with altitude. Conversely, the correlations between IAGOS and GAW stations usually reach a flat maximum at an altitude that roughly corresponds to the elevation of the GAW surface station. For O_3, the correlation between IAGOS and AQN stations is also decreasing with altitude but more progressively.

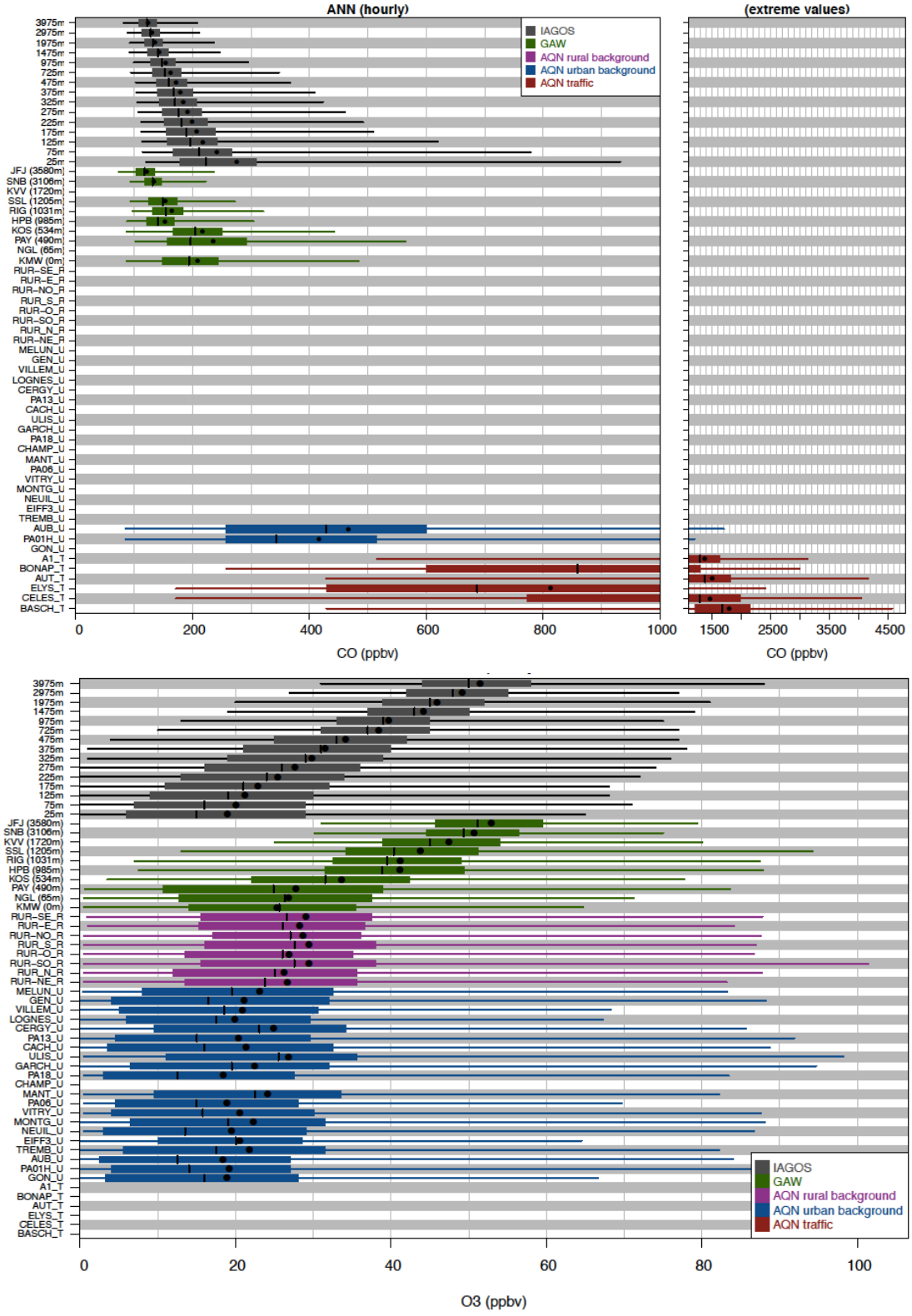

Figure S-11: Distribution of the CO (top panel) and O_3 (bottom panel) hourly mixing ratios at Paris. The Figure shows the 1st, 25th, 50th, 75th and 99th percentiles (box-and-whisker) and the mean (black point). A strong CO pollution is observed at traffic stations. Although much lower, the CO mixing ratios measured at urban background stations remain higher than the mixing ratios observed by IAGOS close to the surface. However, the O_3 mixing ratios measured by IAGOS close to the surface are consistent with the observations at urban and rural background stations. Higher in altitude, IAGOS O_3 observations get closer to the mixing ratios measured at GAW regional stations.

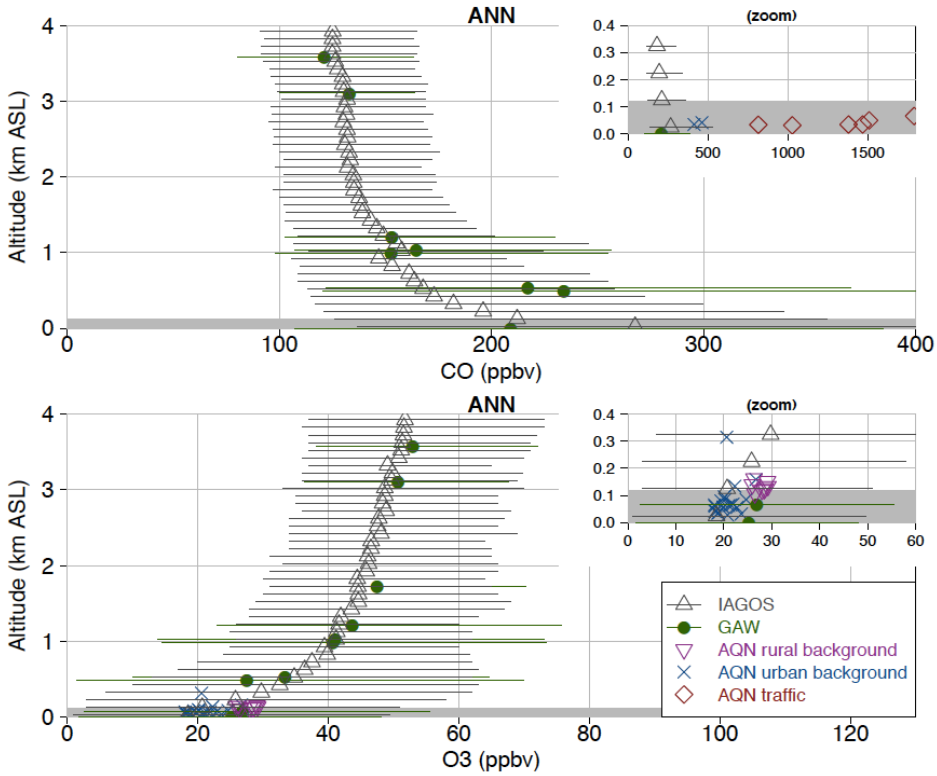

Figure S-12: CO (top panel) and O_3 (bottom panel) mixing ratios versus altitude, as given by IAGOS and surface stations at Paris. The grey area indicates the elevation of the Paris airport (119 m). The Figure shows the mean (points) and the 5th and 95th percentiles (horizontal lines; only for GAW and IAGOS, for clarity). As at Frankfurt and Vienna, a good agreement is found between the different datasets when plotted against altitude.

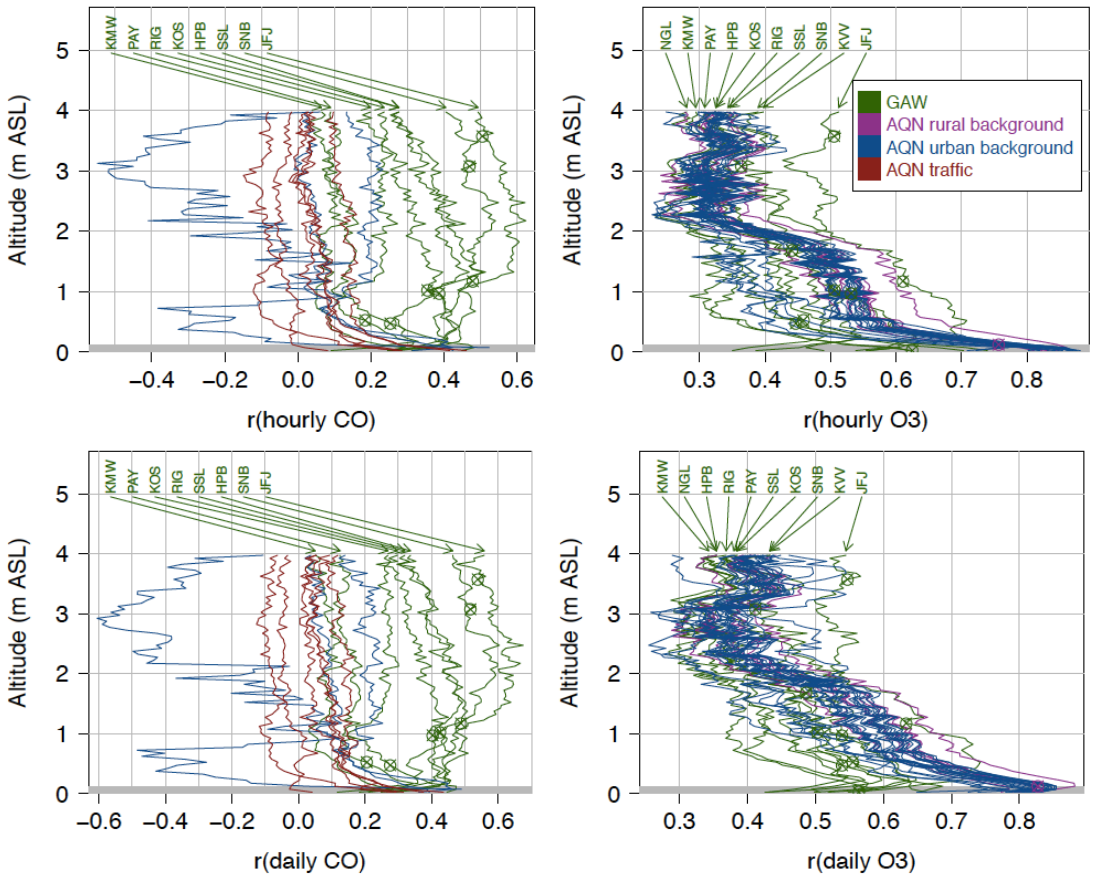

Figure S-13: Correlation between the IAGOS observations at several altitudes and the surface measurements, at Paris. The correlations are calculated for the hourly (top panels) and daily (bottom panels) data, for CO (left panels) and O_3 (right panels). For clarity, only the name of GAW stations is written. For each GAW station and for the rural background station, the elevation is indicated on the corresponding curves by open circles with a cross. The correlation profiles at Paris are more noisy and complex than at Frankfurt and Vienna, which may be partly due to the lower number of data. Although higher close to the surface (with exceptions at a few stations), the correlations on CO between IAGOS and AQN surface stations are very low. They are slightly higher between IAGOS and GAW station in altitude. For O_3, correlations between IAGOS and surface stations are highest close to the surface and decrease with altitude. Contrary to Frankfurt and Vienna, the altitude of maximum correlation on O_3 between IAGOS and GAW usually does not coincide with the elevation of the station. The larger distance between Paris and GAW stations may partly explain these differences.

Table S-1: Description of the surface stations.

City	Station	Location	Elevation
Frankfurt	DEHE052_R	8.4461°E, 50.2219°N	811m
	DERP009_U	8.2740°E, 49.9950°N	110m
	DEHE001_U	8.6646°E, 49.8723°N	158m
	DEHE005_U	8.5421°E, 50.1019°N	104m
	DEHE011_U	8.9181°E, 50.1348°N	106m
	DEHE018_U	8.4515°E, 50.0103°N	90m
	DEHE022_U	8.2449°E, 50.0503°N	121m
	DERP007_U	8.2165°E, 50.0171°N	120m
	DERP008_U	8.2546°E, 50.0104°N	85m
	DEHE008_U	8.7463°E, 50.1253°N	100m
	DEHE037_T	8.2303°E, 50.0772°N	145m
	DEHE041_T	8.6919°E, 50.1246°N	119m
	DERP010_T	8.2613°E, 50.0010°N	85m
	DEHE040_T	8.6537°E, 49.8695°N	158m
	DERP011_T	8.2656°E, 50.0100°N	85m
	DERP012_T	8.2690°E, 49.9988°N	85m
Vienna	AT30302_R	16.6767°E, 48.0508°N	210m
	AT30603_R	16.4333°E, 48.0861°N	172m
	AT32701_U	16.4745°E, 48.1450°N	155m
	AT31401_U	16.3022°E, 48.0861°N	210m
	AT31402_U	16.3317°E, 48.1250°N	194m
	AT30065_U	16.1756°E, 48.2072°N	248m
	AT30201_U	16.2070°E, 47.9600°N	286m
	AT30301_U	16.9611°E, 48.1439°N	165m
	AT30601_U	16.3047°E, 48.3014°N	200m
	AT900ZA_U	16.3578°E, 48.2492°N	207m
	AT90LAA_U	16.3928°E, 48.1614°N	250m
	AT90LOB_U	16.5267°E, 48.1625°N	150m
	AT9JAEG_U	16.2989°E, 48.2711°N	520m
	AT9STEF_U	16.3739°E, 48.2089°N	173m
	AT90MBA_T	16.3020°E, 48.1889°N	195m
	AT90TAB_T	16.3820°E, 48.2181°N	160m
	AT9GAUD_T	16.3406°E, 48.1878°N	175m
	AT9RINN_T	16.4078°E, 48.1850°N	160m
Paris	RUR-SE_R	2.6452°E, 48.3548°N	127m
	RUR-E_R	3.0570°E, 48.7607°N	120m
	RUR-NO_R	1.8664°E, 49.0632°N	122m
	RUR_S_R	2.2352°E, 48.3634°N	134m
	RUR-O_R	1.6768°E, 48.8604°N	107m
	RUR-SO_R	1.8827°E, 48.5823°N	152m
	RUR_N_R	2.3438°E, 49.1003°N	140m
	RUR-NE_R	2.7489°E, 49.0283°N	162m
	MELUN_U	2.6611°E, 48.5422°N	56m
	GEN_U	2.2943°E, 48.9303°N	28m
	VILLEM_U	2.5063°E, 48.8816°N	85m
	LOGNES_U	2.6347°E, 48.8403°N	80m

	CERGY_U	2.0411°E, 49.0460°N	85m
	PA13_U	2.3596°E, 48.8285°N	57m
	CACH_U	2.3296°E, 48.8002°N	63m
	ULIS_U	2.1645°E, 48.6789°N	159m
	GARCH_U	2.1877°E, 48.8464°N	134m
	PA18_U	2.3456°E, 48.8917°N	60m
	CHAMP_U	2.5163°E, 48.8168°N	74m
	MANT_U	1.7033°E, 48.9962°N	32m
	PA06_U	2.3348°E, 48.8483°N	41m
	VITRY_U	2.3757°E, 48.7759°N	95m
	MONTG_U	2.4571°E, 48.7066°N	68m
	NEUIL_U	2.2773°E, 48.8813°N	36m
	EIFF3_U	2.2942°E, 48.8579°N	315m
	TREMB_U	2.5745°E, 48.9555°N	65m
	AUB_U	2.3847°E, 48.9039°N	42m
	PA01H_U	2.3448°E, 48.8622°N	35m
	GON_U	2.4448°E, 48.9909°N	65m
	A1_T	2.3565°E, 48.9252°N	35m
	BONAP_T	2.3345°E, 48.8563°N	32m
	AUT_T	2.2523°E, 48.8502°N	50m
	ELYS_T	2.3116°E, 48.8688°N	34m
	CELES_T	2.3601°E, 48.8526°N	35m
	BASCH_T	2.3267°E, 48.8276°N	66m